Patient-specific Mechanical Simulation of the Knee Joint with Integration of Magnetic Resonance T1-T2 Values

Diego Infante[1], Ricardo Belda[1], Ángel Alberich-Bayarri[2], Roberto Sanz-Requena[3], Luis Martí-Bonmatí[2,3], Eugenio Giner[1]

1 Dpt. of Mechanical Engineering and Materials - CIIM, Polytechnics University of Valencia, Valencia, Spain
2 Biomedical Imaging Research Group (GIBI2^30), La Fe Polytechnis and University Hospital, Valencia, Spain
3 Biomedical Engineering, Quiron Hospitals Group, Valencia, Spain

email: angel@quibim.com

Abstract: Articular cartilage exhibits unique depth-dependent mechanical properties influenced by its heterogeneous composition and inhomogeneous distribution of proteoglicans, water content and collagen fibrils. Recent studies have estimated the mechanical properties of articular cartilage with MRI. The aim of this study is to analyse the importance of these depth-dependent properties for mechanical stresses and strains resulting from the contact simulation between tibial cartilage and femoral cartilage in knee joint. In order to make the model, the mechanical properties were assigned from T1-T2 mapped MR-images. Subject-specific anatomic structures and mechanical properties of femoral and tibial cartilage were implemented in a 3D finite element model extracted from MR images. Cartilage was segmented using a self-developed software from high resolution T1-weighted images obtained in a 3T magnet. Cartilages and bones were modelled as linear isotropic elastic materials, with non-homogeneous properties in the case of cartilage.
Keywords: Articular cartilage, finite elements

Introduction

Articular cartilage is the tissue that covers the bearing surfaces in all synovial joints providing low-friction and allowing free-pain movement [1]. From a mechanical point of view, cartilage is a porous, viscoelastic material [2], which shows anisotropic and nonlinear properties in compression and tension [3], consisting of three phases: 1) a solid phase, which is mainly composed by a collagen fibrillar network (15–22% by wet weight) enmeshed with proteoglycan macromolecules (PG, 4–7% by wet weight; 2) a fluid phase, which is water (80% by wet weight); and 3) an ion phase, which has many ionic species with positive and negative charges.

Composition and structure of articular cartilage vary through depth [4].This way, articular cartilage can be divided into 4 main zones specified by thickness: the superficial, middle, deep and calcified cartilage zone.

Some ex-vivo studies in humans and other species have shown that the load-bearing capacity of cartilage is dependent on the content of their components [5-8]. MR imaging has become a powerful non-invasive technique for exploring the anatomy and function of tissues and organs within the human body. For that reason, some authors have established a connection between magnetic resonance parameters and water content [11], glycosaminoglycan concentration [12] or collagen distribution [13]. For example, Nissi et al. [10] have established relationships between bulk T1 or T2 relaxation time and mechanical properties of the samples.

Furthermore, some authors have found a connection between local mechanical properties and magnetic resonance parameters. We can refer to Samosky et al. [9], who found a high correlation between the dGEMRIC index (T1Gd-) and local stiffness. Consequently, it would be possible that the local stiffness would change according to the composition of the local sample.

This study is aimed at implementing local mechanical properties extracted from mapped MR-images applying the relationship established by Nissi et al. [10] in a 3D non-linear FEM subject-specific of the contact between tibial and femoral cartilage. Results obtained in strain and stress were compared to homogenous and local assignment of the mechanical properties.

Materials and methods

MRI acquisition, segmentation and registration

The image acquisitions were performed in a left knee joint with magnetic resonance 3T Achieva TX scanner (Philips Healthcare, Best, The Netherlands) magnet. Two image acquisitions were carried out for the proper execution of the simulation: 1) a 3D high-spatial resolution set of images for bone and cartilage characterization; and 2) a T1-mapped set of images for parametric material property assignation.

The designed pulse sequence for segmentation image acquisition consisted of a 3D T1 gradient-echo

sequence with water selective excitation (TR=20 ms, TE=4.43 ms, flip angle=15°, slice thickness=1 mm, matrix size=512x512, in-plane resolution= 0.3 mm). On the other hand, image acquisition for T1 mapping consisted of a T1 3D gradient echo (GE) with a varying flip angle (TR=8 ms, TE=4 ms, flip angle=2° to 40º, slice thickness=3 mm, matrix size=192x192, in-plane resolution=0.78 mm).

Articular bones and cartilages were segmented through sagittal planes slice by slice using an in-house developed solution. The tool also allowed the registration of T1 maps in the cartilage geometry. The final results obtained from this tool were a three-dimensional matrix with voxel-wise T1 values of each anatomic component of the simulation.

Material properties

In all simulations, cartilage and bone were modelled as elastic isotropic materials. Elastic materials are completely defined by two constants: Young's modulus and Poisson coefficient. Material properties of bone were extracted from Reily et al [15] (E=17GPa, ν=0.3).

Material properties of cartilage were extracted from Nissi et al. [10] estimation from T1-mapped images. The relationship between T1 relaxation time and Young's modulus is shown in table 1.

Table 1: Relationship between material properties and relaxation time T_1.

T_1 (ms)	E (Pa)
$T_1 < 1328$	$1.03 \cdot 10^6$
$1328 \leq T_1 \leq 2026$	$-1045.85\ T_1 + 1.08 \cdot 10^8$
$T_1 > 2026$	$0.3 \cdot 10^6$

Three different material property mapping were simulated for the study of depth-wise properties in cartilages: a) "HA" Homogeneous Assignation to all elements by mean T1 relaxation time of the whole cartilage; b) "HAT" Homogeneous Assignation to Transversal element planes by mean T1 relaxation time in each transversal sample; and c) "EBEA" Element By Element Assignation extracted from T1-mapped relaxation time.

Meshing of the anatomic structures

All meshes were performed by a free MatLab/octave-based mesh generator iso2mesh [14]. Firstly, binary volumes from segmented mask were slightly smoothed for improving the contact surfaces between components. The following step consisted on extracting an isosurface from the smoothed volumes. Finally the isosurfaces were meshed with tetrahedral elements and the cartilage ones were refined in order to obtain more accurate results.

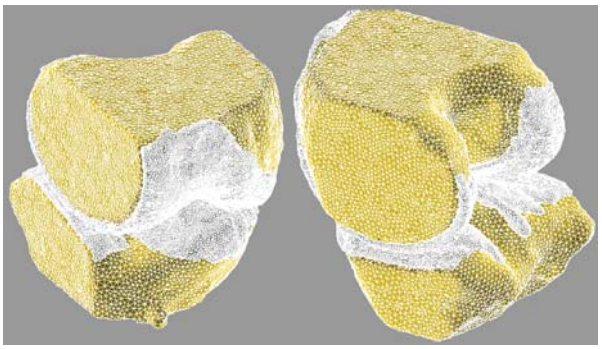

Figure 1: Knee joint mesh generated from MR images.

Boundary conditions and simulations

Exterior nodes located at the bottom face of the tibia were fixed. Exterior nodes located at the top face of the femur were fixed in transversal displacements. However, nodes on the top femur surface were constrained with 1 mm displacement in the longitudinal direction of the bone. The constraints remain unchanged in all simulations.

Numerical solution was performed with the commercial software ANSYS 14.5. (ANSYS Inc, Southpointe, PA, USA). Contact between cartilages was solved with the Augmented Lagrangian method. Contacts between cartilage-bone surfaces were substituted by the multi point constraints (MPC).

Results

Results obtained from the numerical resolution were specially focused on strains and displacement comparing mean values in each cartilage. Stresses were less accurate than displacements due to local high stresses located in the contact between cartilages. Mean displacement values were normalized by the imposed displacement constraint (1 mm) and are presented in Table 2. Mean strain values for cartilages are shown in Table 3.

Table 2: Mean displacement values for each cartilage normalized by the imposed displacement.

	Femoral Cartilage	Tibial Cartilage
HA	0,920	0,224
HTA	0,923	0,220
EBEA	0,924	0,216

Table 3: Mean strain values for each cartilage.

	Femoral Cartilage	Tibial Cartilage
HA	0,0410	0,0525
HTA	0,0421	0,0517
EBEA	0,0425	0,0517

The different results obtained with the methods can be appreciated in table 4 and 5.

Table 4: Relative strains compared to EBEA analysis.

	Femoral Cartilage	Tibial Cartilage
HA	-3,46%	1,41%
HTA	-0,89%	0,01%

Table 5: Relative displacements compared to EBEA analysis.

	Femoral Cartilage	Tibial Cartilage
HA	-0,43%	3,33%
HTA	-0,10%	1,86%

Displacement femoral cartilage distribution for each model is shown in Figure 2 and Figure 3.

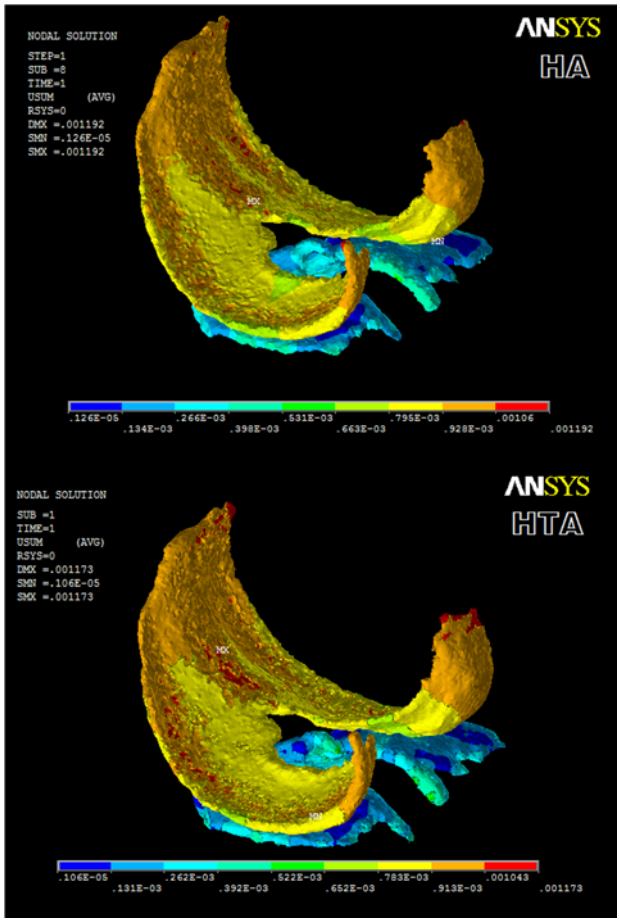

Figure 2: HA and HTA displacement vector sum distribution.

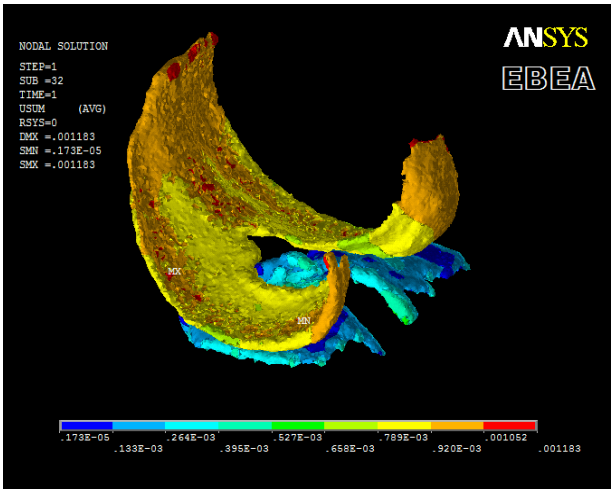

Figure 3: EBEA displacement vector sum distribution.

Discussion

Analysing mean strain results globally, strains in Tibial cartilage are approximately 25% higher than in Femoral cartilage, so Tibial cartilage is the component that suffer greater levels of stresses. A discussion of relative strains compared to the EBEA model is presented in Table 4. Relative strain results for EBEA are higher for Femoral cartilage than HA and HTA results and lower for Tibial cartilage than HA and HTA results. Furthermore, differences between HTA and EBEA assignation are practically negligible (lower than 1%), so it can be concluded that EBEA and HTA models lead to similar results in mean strains for each cartilage.

A discussion of relative displacements compared to EBEA analysis is presented in Table 5. The tendency in relative strain results is also observed in relative displacement results. EBEA model produces higher mean displacement for Femoral cartilage than HA and HTA models, and lower mean displacement results for Tibial cartilage.

Analysing the results in Table 5, we can claim that relative mean displacement are nearly the same in Femoral cartilage for each model (differences are lower than 0.5%). Tibial cartilage mean displacement results for EBEA model are lower than results predicted for HA and HTA models but differences are lower than 3,5%. Furthermore, local assignations of the mechanical properties were responsible of the variations in the displacement distribution shown in Figure 2.

To conclude, Tibial cartilage suffers greater stress level so is the most critical component. In terms of mean strain and displacement values, EBEA, HTA and HA models predict similar results. The difference between using each model is lower than 3,5% in any case so we can conclude that using a simpler model produce a low level of error in terms of mean values for each cartilage. Nevertheless, EBEA results should be

experimentally validated. In order to improve local results which allow quantifying local stresses and strains, geometric discontinuities should be removed.

References

[1] Buckwalter JA, Mankin HJ, Grodzinsky AJ. Articular cartilage and osteoarthritis. AAOS Instructional Course Lectures. 2005; 54: 465–80.
[2] Lu XL, Mow VC. Biomechanics of Articular Cartilage and Determination of Material Properties. Med. Sci. Sports Exerc. 2008; 40 (2): 193–99.
[3] Boschetti F, Pennati G. Biomechanical properties of human articular cartilage under compressive loads. Biorheology. 2004; 41: 159-166.
[4] Hunziker E.B., Quinn T.M., Häuselmann H.-J. Quantitative structural organization of normal adult human articular cartilage. Osteoarthr Cartil. 2002; 10: 564–72.
[5] Allen RG. Mechanical properties of selectively degraded cartilage explants: correlation to the spatiotemporal distribution of glycosaminoglycans. In: Mechanical engineering. Cambridge: Massachusetts Institute of Technology; 1996.
[6] Armstrong CG, Mow VC. Variations in the intrinsic mechanical properties of human articular cartilage with age, degeneration, and water content. J Bone Jnt Surg Am. 1982; 64: 88-94.
[7] Harris Jr ED, Parker HG, Radin EL, Krane SM. Effects of proteolytic enzymes on structural and mechanical properties of cartilage. Arthritis Rheum 1972; 15: 497-503.
[8] Jurvelin JS, Arokoski JP, Hunziker EB, Helminen HJ. Topographical variation of the elastic properties of articular cartilage in the canine knee. J Biomech 2000; 33: 669-75.
[9] Samosky JT, Burstein D. Spatially-localized correlation of dGEMRIC-measured GAG distribution and mechanical stiffness in the human tibial plateau. Journal of Orthopaedic Research. 2005; 23:93-101.
[10] Nissi M, Rieppo J. Estimation of mechanical properties of articular cartilage. OsteoArthritis and Cartilage. 2007; 15: 1141-1148.
[11] Liess C, Lüsse S, Karger N. Detection of changes in cartilage water content using MRI T2-mapping in vivo. Osteoarthritis and Cartilage. 2002; 10: 907–913.
[12] Burstein D, Gray ML. Potential of molecular imaging of cartilage. Sports Medicine Arthrosc Rev. 2003; 11: 182-91.
[13] Nieminen MT, Rieppo J, Toyras J, Hakumaki JM, Silvennoinen J, Hyttinen MM. T2 relaxation reveals spatial collagen architecture in articular cartilage: a comparative quantitative MRI and polarized light microscopic study. Magn Reson Med. 2001; 46 (3): 487–93.
[14] Qianqian F, Boas David. Tetrahedral mesh generation from volumetric binary and gray-scale images. Proceedings of IEEE International Symposium on Biomedical Imaging. 2009; 142-1145
[15] Reilly DT, Burstein AH. The mechanical properties of bone. J. Bone Joint Surg. Am. 1974; 56: 1001.